# Dynamics of entropy wave generation in a simplified model of gas turbine combustor: A theoretical investigation

Abolfazl Fattahi[1*], Nader Karimi[2,3], Najmeh Hajialigol[4]
[1]Department of Mechanical Engineering, University of Kashan, Kashan 8731753153, Iran
[2]School of Engineering and Materials Science, Queen Mary University of London, London E1 4NS, United Kingdom
[3]James Watt School of Engineering, University of Glasgow, Glasgow G12 8QQ, United Kingdom
[4]Department of Mechanical Engineering, Tarbiat Modares University, Jalal AleAhmad, Nasr, Tehran 1411956512, Iran
*The corresponding author, afattahi@kashanu.ac.ir

**Abstract** Entropy noise remains as a largely unexplored mechanism of combustion generated noise. Currently, little is known about the production sources of entropy waves in flames. To address this issue, the present work puts forward a theoretical investigation of the generation of entropy waves in a one-dimensional, ducted flow. A linear theory is developed for the dynamic responses of different sources of unsteady entropy generation including thermal, hydrodynamic, pressure and chemical irreversibility. For the first time in literature, dynamics of chemical sources of unsteady entropy generation are investigated extensively. It is found that the mixture fraction fluctuations are responsible for the production of almost all unsteady chemical entropy and that the effect of chemical potential is negligibly small. For the Strouhal numbers less than unity, fluctuations in pressure are the most significant source of the overall generation of unsteady entropy. However, at higher frequencies, mixture fraction fluctuations dominate the generation of entropy wave. The cut-off frequency for the generation of entropy wave is shown to depend not only on the thermal and hydrodynamic characteristics of the flame, but also on the chemical properties of the downstream gases. It is further argued that the transfer function of entropy generation for a thin flame may feature an unrealistically high amplitude. This study shows that neglecting the chemical sources of entropy wave can result in wrong predictions of the combustor acoustics and impede suppression of combustion instabilities and noise.

**Key words:** Thermoacoustic instabilities; Indirect Combustion noise; Entropy waves; Compositional inhomogeneities.

| **Nomenclature** | | | |
|---|---|---|---|
| $cp$ | Specific heat constant (kJ/kgK) | | Chemical potential (kJ/kmol) |
| $\mathcal{D}$ | Mass diffusivity (m2/s) | $\Delta$ | Flame length (m) |
| $E$ | Total energy (kJ) | $\Psi$ | Chemical potential function (-) |
| | Internal energy per mass (kJ/kg) | $\gamma=cp/cv$ | Heat capacity ratio (-) |
| | Body force (kN) | $\lambda$ | Acoustic wavelength (m) |

| | | | |
|---|---|---|---|
| $k$ | Thermal conductivity (kJ/kgK) | $\xi$ | Distance from flame (m) |
| $Le$ | Lewis number | | Density (kg/m3) |
| $MWi$ | Molar mass (kg/kmol) | $\boldsymbol{\alpha}$ | Thermal diffusivity (m2/s) |
| | Pressure (Pa) | $\upsilon$ | kinematic viscosity (m2/s) |
| $R$ | Gas constant (kJ/kg/K) | $\omega$ | Angular frequency (2π/s) |
| $Re$ | Reynolds number (-) | $\phi$ | Entropic transfer function (-) |
| | Heat addition rate per unit volume (kJ/sm3) | **Superscripts** | |
| $q$ | Heat flux ((kJ/sm2) | ' | Temporal part |
| $Q$ | Heat release (kJ) | 0 | Standard status |
| $s$ | Entropy per unit mass (kJ/kgK) | **Subscripts** | |
| | Time (s) | 1 | Flame upstream |
| $T$ | Temperature (K) | 2 | Flame downstream |
| $u$ | Velocity (m/s) | $c$ | Chemical |
| $uD,i$ | Flow diffusive velocity (m/s) | $h$ | Thermal |
| $Yi$ | Mass fraction (-) | $m$ | Mean |
| $Z$ | Mixture fraction (-) | $p$ | Fluctuated |
| **Greek symbols** | | $u$ | Universal |

## 1. Introduction

The aero-engine core noise is now a major environmental concern, particularly at low-power engine conditions during approach and landing [1]. Mitigation of the core noise has gained an increasing attention as the latest European regulatory strategy aims to reduce the noise at its inception [1]. The core noise can be broadly divided into self-noise, as the direct generation of acoustic waves by the engine components, and that associated with the induced noise, produced by the flow inhomogeneities [2,3,4]. The main purpose of the current study is to understand the dynamics of generation of those flow inhomogeneities that are of chemical composition nature.

It is now well-established that combustion noise is the second powerful source of noise emission in the aero-engines after fan and jet noise [5]. Despite subsiding the aerodynamic sources of noise by employing ultra-high bypass ratio turbofan engines and aerodynamic optimization, the core noise has been continuously bound to increase [1,6]. This is primarily due to the intensification of combustion noise in low-pollution combustors, which are currently in extensive use [6-8]. Direct combustion noise is associated with flame fluctuations induced by the interactions between flow turbulence and combustion process [9,10]. However, indirect combustion noise is generated downstream of the flame as inhomogeneities in the flow, e.g. velocity, pressure, temperature and mixture composition, pass through a region of mean pressure gradient [1,3,11,12]. Such inhomogeneities are collectively referred to as entropy waves, and are usually produced in the reactive region of the flow. Nonetheless, their conversion to sound often occurs at the exit nozzle or first stage of the turbine stator [13,14]. Once either of direct or indirect combustion noise is generated, the

resultant acoustic wave can contribute to the core noise by propagating out of the engine. Further, the reflected acoustic waves may trigger thermoacoustic combustion instability, characterized by destructive, large-amplitude pressure fluctuations [1,15,16]. Despite verification of its contribution to combustion instability and noise emission, indirect combustion noise is still the lesser understood mechanism of sound generation in gas turbine combustors [16-23]. This could be due to the intricate physics and the complex interactions of entropy waves with the flow and thermal fields [13].

Conversion of entropy waves to sound by passing through nozzles has been the subject of several analytical, numerical and experimental studies. The compact-nozzle theory [3] based on a one-dimensional and linear analysis has been traditionally the key method for calculating the acoustic conversion of entropy waves. In recent years, some subsequent efforts have been made to extent the analysis and relax the assumptions made in Ref. [3]. These include implementation of the effective nozzle-length method [24, 25], linear nozzle element techniques [26, 27] and expansion methods [28]. Compact nozzle theories have been also developed for the low frequency range of entropy noise through a non-isentropic nozzle with pressure losses [29] and spatially decaying and stretching entropy waves [30]. It is important to note that most previous numerical and theoretical studies on entropy waves were carried out on the basis of Euler equations [24,24,31]. Due to the absence of diffusion, these equations are unable to fully simulate the generation and decay of entropy waves. A series of experimental analyses on the conversion of entropy noise were provided by Bake et al. [32,33]. Using a similar set-up, Domenico et al. [29] separated direct and indirect reflective noise upstream of the nozzle. Yet, none of these experimental studies were focused on the production or annihilation of entropy waves.

Recently, large eddy simulations in simplified geometries [34,35], convergent-divergent nozzles [36] and real combustors [37] provided further information on the propagation of entropy waves. For example, several investigations indicated that entropy waves are annihilated during downstream advection [19,38,39,40]. However, other studies asserted that the entropy waves could readily reach the exit nozzle of combustor [41,42]. Fattahi et al. [34] showed that the contradicting conclusions arise from the thermal boundaries and hydrodynamic conditions of the combustors and both sets of conclusions could be valid. Further, in their experimental study, Hosseinalipour et al. [43] predicted the decay dynamics of entropy waves by comparing the wavelength and the characteristic length of the combustor. Most recently, Christodoulou et al. [44] developed a low-order dynamical model to predict the evolution of entropy waves based on the high-order computation of the early stages of wave propagation. These works shed some light on the spatiotemporal dynamics of entropy wave propagation in combustors. Nevertheless, they were entirely concerned with hot spots or temperature disturbances as entropy waves and ignored other possible sources of entropy perturbations. More importantly, they excluded the generation of entropy waves.

In 1970’s, Sinai [45] introduced a novel extra source of entropy disturbances and indirect noise. He extended Lighthill analogy and showed that convection of a chemical blob in a steady and

low Mach number flow could produce sound [46]. A much more recent attempt was made by Magri et al. [47] to formulate the indirect noise of inhomogeneities in mixture composition or the so-called ‘compositional noise’. These authors extended the compact nozzle theory for a multi-component gas mixture. It was found that compositional noise is strongly depended on the mixture composition and could exceed direct and conventional entropy noise for supercritical nozzles. Magri et al. [48] also calculated the indirect compositional noise by relaxing the compact nozzle assumption for Helmholtz number up to 2 and showed that the compact theory overestimates the indirect noise. Rolland et al. [49] measured compositional noise produced by injection of helium into an airflow and reported good agreement with the theory of Magri et al. [47]. In addition, indirect compositional noise in a Rolls-Royce combustor engine was investigated by Guisti et al. [50] revealing that oxygen, water and carbon dioxide are respectively the most dominant sources of compositional noise. This study concluded that compositional inhomogeneities are a non-negligible source of noise [50].

Although the general area of indirect combustion noise has received some attention, the production sources of entropy wave in flames are still largely unexplored. In an early work, Bloxsidge et al. [51] presented a differential equation, containing unsteady heat release, pressure and velocity fluctuations as the sources of entropy waves. Assuming a compact flame, Dowling [52] presented a more precise equation in which heat release rate and velocity were the dominant sources of unsteady entropy generation in the flame. Later, Karimi et al. [53] showed that the equations derived by Bloxsidge et al. [51] and Dowling [52] act as a low-pass filter with a floating corner frequency. Numerical solutions of mass, momentum and energy at both sides of the flame were conducted to determine the strength of entropy waves [54,55]. Further, Dowling and Mahmoudi [4] showed that fluctuations of heat and mass flow rate act as the source of entropy wave in the flame region. However, Chen et al. [56,57] argued against the assumption of stationary flame front to derive sources of entropy wave. They claimed that in a perfectly premixed flame, the heat release is the only source of unsteady entropy generation with low amplitude.

Clearly, these findings are scattered and do not provide a coherent view on the generation mechanisms of entropy waves in gas turbine combustors. Nonetheless, suppression of the core noise requires an in-depth understanding of the generation of the entropy wave formed by thermal, hydrodynamic and chemical inhomogeneities. Under the assumption of linearity, this is provided by a transfer function, which relates the production of entropy waves to various flow disturbances. In a recent theoretical study, Yoon [58] analytically derived such transfer function immediately downstream of the flame. Importantly, however, only non-chemical sources under Eulerian flow assumptions were considered in that work [58]. To release this limitation, the current study aims to capture all sources of entropy wave in the flame region. The transfer functions for the chemical entropy wave immediately downstream of the flame are derived analytically. Zero flame length, commonly used in the earlier related studies, is avoided as this assumption overestimates the strength and frequency content of the entropy wave [58].

## 2. Governing equations

The investigated configuration includes a plain one-dimensional channel, formed between two parallel plates, as shown in Fig. 1.

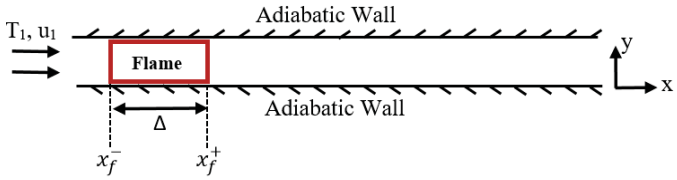


Fig. 1. The schematic configuration used in the current study.

The inlet temperature and pressure of the flow without entropy wave is respectively 300K and 1bar. The channel is adiabatic with the inlet Reynolds number of *1000* based on the channel height and bulk flow velocity.

The governing equations correspond to a one-dimensional, continuous flow in a duct with an arbitrary cross section and length. The flame heat release is limited to a narrow interval of $[xf-,xf+]$. Considering two known and different velocities at the flame upstream ($xf-$) and downstream ($xf+$), there is no need to solve the momentum equation. The following assumptions are made throughout the proceeding analysis.

- The flow is laminar.
- Thermophysical properties of the fluid are constant and time-independent.
- The investigated flow includes a diffusion flame.
- The analysis holds for single-step, infinitely fast chemistry (Shvab-Zeldovich limit) [59].
- Soret and Dufour effects are negligible.
- The gaseous mixture is ideal and calorifically perfect.
- All constituent species have equal diffusivities.

The general form of energy equation is [9]

$$\rho DeDt=-\nabla.q+\nabla.(pu)+\nabla.(u.\tau)+\rho i=1NYi(u+uD,i).Fi, \quad (1)$$

where the last three terms on the right hand side are respectively related to work done on the fluid at the surfaces by pressure, viscous and body forces. Using Gibbs equation (Eq. (2)), the material derivative of entropy is presented in Eq. (3).

$$de=Tds+pd\rho\rho2-i=1N\mu iMWidYi, \quad (2)$$

$$TDsDt=DeDt-p\rho2D\rho Dt-i=1N\mu iMWiDYiDt. \quad (3)$$

Substituting Eq. (3) into Eq. (1) and neglecting the viscous and body forces, the energy equation in terms of entropy is extracted. After some algebraic manipulations, this reduces to

$$TDsDt=-q\rho-i=1N\mu iMWiDYiDt, \quad (4)$$

in which, $T$, $s$, $\rho$ and $q$ are, respectively, temperature (K), entropy per unit mass (kJ/kgK), density (kg/m3) and rate of heat addition per unit volume (kJ/m3s). Further, $\mu i$ is the chemical potential (kJ/kmol), $Yi$ mass fraction (-) and $MWi$ molar mass (kg/kmol) of $i$th species in a mixture containing $N$ chemical components.

Considering mass fraction of the species as a single function of mixture fraction in a diffusion flame with infinitely fast chemistry [47,59] and utilizing the chain rule of differentiation, the material derivative of mass fraction of each species becomes,

$$DYiDt=DYiDZDZDt, \quad (5)$$

where $Z$ is the mixture fraction. Setting $\xi=x-xf-$ as the coordinate translation and assuming the exponential variation of density and mixture fraction across the flame,

$$d\rho d\xi=-\kappa\rho, dZd\xi=-\beta Z, \quad (6)$$

the distributions of density and mixture fraction are given by

$$\rho=\rho 1\exp(-\kappa\xi), Z=Z1\exp(-\beta\xi), \quad (7)$$

where the index 1 denotes the variable at the flame initiation position. It is worth noting that by proper curve fitting on the kinetic results of mass fractions, derived by USC-Mech II [60], the exponential variation of mass fraction was verified in the narrow region of the n-dodecane-air flame. For the flow under investigation, a linear relation exists between the mixture fraction and mass fraction [59]. Therefore, the spatial variation of mixture fraction is also assumed to be exponential. Further, a curve fitting allows for the exponential variation of density across the flame to be derived from the work of Yoon [58].

Invoking the assumption of equal diffusivities ($\mathcal{D}$ $(m2/s)$), the governing equation for the mixture fraction is given by [9]

$$\rho\partial Z\partial t+\rho u.\nabla Z-\nabla.(\rho\mathcal{D}\nabla Z)=0. \quad (8)$$

Considering the definition of material derivative, Eq. (8) is re-written as

$$\rho DZDt-\nabla.(\rho \mathcal{D}\nabla Z)=0. \tag{9}$$

Applying the definition of chemical potential (Ψ), presented in Eq. (10), and combining Eqs. (5) to (7) with (9), the energy equation is finally turned into Eq. (11).

$$\Psi=1Tcp1N(\mu i/MWi)dYidZ, \tag{10}$$

$$DsDt=q\rho T-cp\Psi \mathcal{D}(\beta 2Z+\kappa\beta Z). \tag{11}$$

In Eq. (11), $u$, involved in the material derivative, is the longitudinal flow velocity (m/s) and $cp$ is the heat capacity (kJ/kgK).

Decomposing entropy disturbance into two parts of thermal ($s\hbar$) and chemical ($sc$) yields

$$Ds\hbar Dt=q\rho T, \tag{12}$$

$$DscDt=-cp\Psi \mathcal{D}(\beta 2Z+\kappa\beta Z). \tag{13}$$

Substituting the flow variables, $g$, by the summation of steady and perturbation parts, such that $g=g+g'$ and neglecting the second order terms, the linearized equation for the transport of entropy is expressed by

$$DsDt=Ds\hbar Dt+DscDt=qpR(q'q+R'R-u'u-p'p)-cp \mathcal{D}(\beta 2+\kappa\beta)\Psi Z(\Psi'\Psi+Z'Z-u'u). \tag{14}$$

Eq. (14) clearly shows all sources of entropy wave generation. According to this equation, fluctuations in thermal, velocity and chemical properties of the flow can lead to the generation of entropy waves.

Dividing both sides of Eq. (14) by $u$ and using an elementary differential identity, the following more compact form of the linearized transport equation of entropy disturbances is obtained.

$$1u\partial s'\partial t+\partial s'\partial x=(qRpu)'-cp \mathcal{D}(\beta 2+\kappa\beta)\Psi Z(\Psi Zu)'. \tag{15}$$

The first source term of Eq. (15) is similar to that derived by Yoon [58], being $qA/m$ for the constant temperature distribution in a duct with the cross sectional area of $A$ and mass flow rate of $m$. Fluctuations of the gas mixture constant due to mixing process can further produce entropy disturbances. The second source term shows the contribution of chemical inhomogeneities with the unsteady generation of entropy. It is inferred from this term that the chemical production of entropy wave does not exist when $\Psi Z=c.u$, where $c$ is a constant. Importantly, this term illustrates the role of flow velocity fluctuations in the generation of chemical part of an entropy wave. Chemical entropy disturbance may exist even under zero fluctuations of mixture fraction and chemical potential, if their mean values are non-zero and the flow contains velocity perturbations. Such condition can be readily encountered in the post flame region of a combustor in which acoustic waves propagate. Further, Eqs. (10) and (11) indicate that in addition to the mixture fraction variation, the chemical potential fluctuation can be another source of chemical entropy wave. It should be noted that this is different to the source of chemical entropy wave presented by Magri et al. [47]. As the chemical potential is dependent on the fluid temperature, $\mu i=\mu i0+RuTln(pi/p0)$ [47], a fluid flow with no variation in mixture fraction but encountering temperature fluctuations can be an example of this source.

As expected, in the limit of negligibly small diffusion coefficient, the chemical entropy generation approaches zero (see Eq. (13)). This is because no Lagrangian variation in the mixture fraction, i.e. $DZDt=0$ (see Eq. (9)), cancels the variations of steady and unsteady parts of $Z$. This also indicates $dYidZ=0$, due to linear relation between $Yi$ and $Z$, causing $\Psi=0$ (see Eq. (10)). Therefore, all chemical sources of entropy generation become ineffective.

## 3. Solution of the transport equation of unsteady entropy

In this section, the transfer function of entropy wave decompositions is derived analytically. Here, subscripts 1 and 2 respectively denote the conditions before and after the flame. Further, it is assumed that the flame heat release includes steady and unsteady components [58],

$$q'(x,t)=qx'(x).qt'(t), \tag{16}$$

with uniform distribution on the flame length, $\Delta=xf+-xf-$,

$$q(x)Qm=q'(x)Qp=1\Delta. \tag{17}$$

Additionally,

$$Qm=xf-xf+q(x)dx,Qp=xf-xf+q'(x)dx,Qm=cp\rho 1u1(T2-T1). \tag{18}$$

It is also assumed that the steady pressure remains constant across the flame [58], as the flow is low-Mach number. That is

$$p(x)=p1=p2. \tag{19}$$

Before commencing the solution process, the following assumptions are further made.

- The flame is acoustically compact, implying $\Delta \ll \lambda acoustics$.
- Gas mixture constant, $R$, is assumed to remain steady. This assumption in conjugation with the constancy of specific heat capacity yields,

$$Rcp=\gamma-1\gamma=1\eta. \tag{20}$$

- Assuming a constant mean heat release, $Qm$, a linear relation between the temperatures at the upstream and downstream of the flame can be found. Further, for an exponential density distribution, the numerical solution of the governing equations across the flame region also gives a linear velocity variation (see Eq. (7)) [58]. Considering the linear velocity and temperature distributions across the flame and assuming $u2=mu1$ and $T2=\alpha T1$, it follows that

$$u(\xi)=(m-1)u1\Delta\xi+u1=r\xi+u1, T(\xi)=(\alpha-1)T1\Delta\xi+T1=f\xi+T1. \tag{21}$$

According to Magri et al. [47,48], the slope of variation of the specific Gibbs energy of the mixture is constant at a narrow range of mixture fraction. Thus,

$$\Psi=1cpT\partial g\partial Z=ecp(f\xi+T1). \tag{22}$$

Applying Laplace transformation on Eq. (14) with an initial condition of $s'\xi,0=0$ results in an ordinary non-linear differential equation for entropy disturbance. This reads

$$1us s'+ds'dx=Au(\xi)+Bu2(\xi), \tag{23}$$

in which

$$A=-QpRp\Delta q'(s)QmRp2p'-cp\mathcal{D}(\beta 2+\kappa\beta)(\Psi' Z+Z'\Psi), B=-QmR\Delta pu'+cp\mathcal{D}(\beta 2+\kappa\beta)\Psi Zu'. \tag{24}$$

Solving the differential Eq. (23) (Bernoulli's type for $n=0$) gives an algebraic equation for the unsteady part of the entropy wave, $s'$, which can be written as

$$s'e\int su(\xi)d\xi=\int(Au(\xi)+Bu2(\xi))e\int su(\xi)d\xi d\xi+C. \tag{25}$$

By substituting $A$ and $B$ from Eq. (24) into Eq. (25) and some algebraic manipulations, the entropy wave at the flame exit, $\xi=\Delta$, can be obtained as follows.

$$s'1cp=Qpq'(s)\eta p1u11m-11-m-s/rsr-\alpha-1(m-1)s/r(1-m-s/r)p1'p1+[-\alpha-1m-1+1p1\eta+\Psi 1Z1\mathcal{D}r(\beta 2+\kappa\beta)][m-1-m-s/rs/r-1+(\kappa-fT1)(1-m-s/rsu1-m-1-m-s/r(s/r-1)(r/u1))]u1'u1, \quad (26)$$

$$s'2cp=(\mathcal{D}(\beta+\kappa)Z1u1)(\beta u1)[1s(1-m-s/r)-\beta u1r2(m-1-m-s/rs/r+1-1-m-s/rsr)]\Psi'(s) + \Psi 1\mathcal{D}r[m-s/r-1sr+fT1(m-m-s/r(s/r+1)(r/u1)-1-m-s/r(s/u1))]Z'(s). \quad (27)$$

The viscous and body forces in the momentum equation and their effects on energy equation are ignored. Further, the gas constant, $R$, and the specific heat constant, $cp$, of the mixture across the flame zone are assumed to be steady. These allow for finding a relation between the velocity and temperature fields [58].

$$u(x)-u1=\gamma-1\gamma p-\rho u2xf-xQm\Delta dx=\gamma-1(\gamma p-\rho u2)\Delta xf-xcp\rho 1u1(T-T1)dx. \quad (28)$$

Assuming low values for the square of Mach number, i.e. $\gamma p \gg \rho u2$, Eq. (28) yields $m=\alpha$.

Transfer functions of the entropy wave decompositions are, therefore, given by the following expressions.

$$\phi h=s'1cpQpq'(s)\eta p1u1=1m-11-m-s/rsr, \quad (29)$$

$$\phi p=s'1cpp1'p1=-(1-m-s/r)sr+(\kappa-fT1)(m-m-s/r(s/r+1)(r/u1)-1-m-s/r(s/u1)), \quad (30)$$

$$\phi u=s'1cpu1'u1(1p1\eta+\Psi 1Z1\mathcal{D}r\beta 2+\kappa\beta)=1m-11-m-s/rsr+(\kappa-fT1)(m-m-s/r(m-1)(s/r+1)(r/u1) -1-m-s/r(m-1)(s/r)(r/u1)), \quad (31)$$

$$\phi\Psi=s'2cp(\mathcal{D}(\beta+\kappa)Z1u1)(\beta u1)\Psi'(s)=\beta u1[1s(1-m-s/r)-\beta u1r2(m-1-m-s/rs/r+1-1-m-s/rsr) ], \quad (32)$$

$$\phi Z=s'2cp\Psi 1\mathcal{D}rZ'(s)=m-s/r-1sr+fT1(m-m-s/r(s/r+1)(r/u1)-1-m-s/r(s/u1)), \quad (33)$$

where subscripts $h$, $p$, $u$, $\Psi$ and $Z$ correspondingly denote heat release, pressure, velocity, chemical potential and mixture fraction.

### 3.1. Transfer functions stability

The values of poles and zeros of a system determine whether the system is stable, or how the system treats instability. All the transfer functions given in Eqs. (29)-(33) have their own poles and zeros. However, after pole-zero cancellation they turn into the functions with no common poles and zeros. Therefore, the zero values of the transfer function are of high importance for the system stability. Substituting the investigated case parameters into all transfer functions shows that the transfer function of velocity ($\phi u$) has a zero with a positive real part, called non-minimum phase transfer function. This type of transfer function arises significant stability concerns in the control theory [61], as it can potentially induce a feedback instability [62]. This indicates that the entropy waves generated by velocity fluctuations are reflected back to the combustor, stimulate velocity or chemical potential fluctuations and launch the feedback loop of combustion instability [38,63]. The same conclusion holds for the real parts of the poles.

## 4. Validation

The noise produced by compositional part of entropy wave has been introduced quite recently [48] and there is still no adequate experimental data to validate the current analysis against. Further, to calculate the chemical transfer functions, chemical potential function of the combustion product components should be primarily accessible. Yet, such information can be rarely found. The exceptions are the limited works of Magri et al. [47,48], which involved chemical data for n-dodecane. However, no transfer functions for chemical decompositions of the entropy wave were presented in those works. Therefore, the current analytical results are compared against the numerical simulations of the entropy wave in the same configuration shown in Fig.1. Appendix A provides the details of the conducted numerical simulations. Further, as shown in Appendix B, all the non-chemical transfer functions ($\phi h$, $\phi p$ and $\phi u$) in the current study can be systematically reduced to those presented by Yoon [58] under the Eulerian flow assumption.

To generate the entropy wave in the numerical simulation (Appendix A), a pocket of products of n-dodecane with different velocity, temperature and pressure compared to the base flow enters the domain depicted in Fig. 1. The ratio between the amplitude of fluctuations and mean values for non-chemical incoming decompositions is held at 30 percent, while the chemical divisions depended on the product mixture composition, varying by the excess air values. Applying Parseval's theorem [64], Eq. (34) defines the energy of a continuous signal, $f$, in the time domain at the first equality and,

frequency domain at the second equality. In the current study, energy of the entropy wave was calculated using Eq. (34) by setting the integration intervals between $-1000\pi$ and $1000\pi$.

$$E=-\infty+\infty|f(xf+,t)|2dt=12\pi-\infty+\infty|F(xf+,j\omega)|2d\omega. \quad (34)$$

The energy of entropy wave, which is a summation of energy of all decompositions, namely velocity ($\phi u$), pressure ($\phi p$), heat release ($\phi \dot{h}$) and chemical parts ($\phi Z$ and $\phi\Psi$), was calculated. Fig. 2 shows a comparison between the numerical and analytical results for three different excess air values. Evidently, there is a good agreement between the two datasets with an average difference of less than 10 percent. This small disparity arises from the simplifications in one-dimensional flow field, numerical errors and the assumptions made to enable analytical solution of the differential equations. The contents of Fig. 2 along with the analytical comparison with the work of Yoon [58] (shown in Appendix B) confirm validity of the analytical derivations presented in Sections 2 and 3. It should be noted that to provide a clear means of comparison, the flame lengths are given the same values as those in the work of Yoon [58]. However, we note that this was termed flame thickness in Ref. [58].

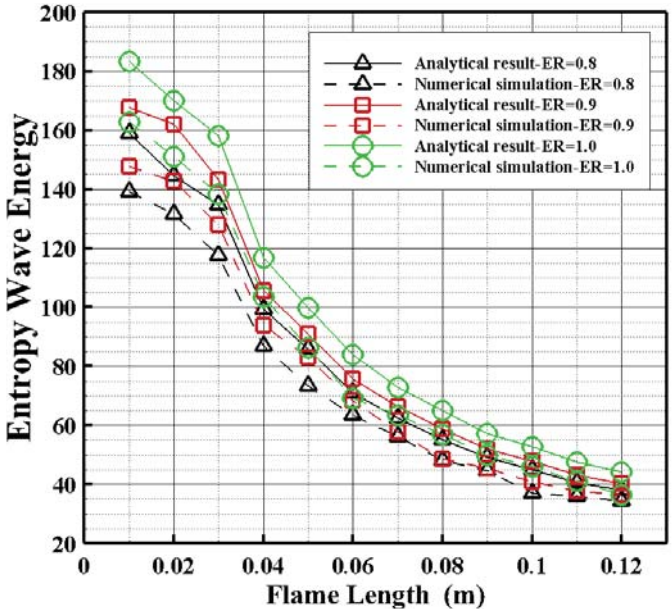


Fig. 2. The energy of entropy wave versus flame length for three excess air values of 0,12% and 25%: comparison between the analytical result and numerical simulation.

## 5. Results and discussions

As stated earlier, the flame zone in Fig. 1 is considered as a narrow region generating the products of complete combustion of a mixture of air and n-dodecane (C12H26), a surrogate of Kerosene. This region includes a spatial gradient of temperature, heat addition, density, mixture

fraction and chemical potential (see Eqs. (7), (17), (21) and (22)). The chemical properties of the mixture were taken from Ref. [48] for three excess air values of 25%, 12% and 0. The physical and chemical properties of the flame region also vary with the changes in excess air. For instance, the ratio between the mean temperature immediately downstream and upstream of the flame, (T2T1), will be 6.623, 6.714 and 6.880, respectively for the stated values of excess air. These temperature ratios were chosen from the numerical results of Magri et al. [47,48] for an infinitesimal dissipation rate n-dodecane-air flame. This is because the flames that generate entropy waves are usually affected by large perturbations. These values subsequently make changes in the mean heat addition to the flow field in accordance with $Qm=cp\rho 1u1T1(\alpha-1)$. However, the mean value of the heat release fluctuation is considered to be constant at $Qp=1kW/m2$ for all values of excess air. The flame length (see Fig. 1) is assumed to be 0.04m and the mixture fraction under stoichiometric condition ($Zst$) is 0.063 [48]. Further, the mean upstream temperature ($T1$) and mean pressure ($p$) at the flame zone are 300K and $1.01\times105$ Pa.

For graphical presentation of the results, a non-dimensional frequency or Strouhal number ($St$) is introduced based on the length of the flame zone ($\Delta$) and mean inlet flow velocity ($u1$):

$$St=\omega\Delta 2\pi u1, \tag{35}$$

where $\omega$ is the angular frequency ($rad/s$) and $\boldsymbol{s}=j\omega$. Fig. 3 shows the magnitude and phase of the transfer functions of entropy wave decompositions (Eqs. (29)-(33)) versus Strouhal number for three different vales of excess air. In keeping with the previous studies [58], Fig. 3 depicts the low-pass filter characteristic of all transfer functions [38, 65, 66 67]. Clearly, as the Strouhal number increases, the amplitude of the transfer functions diminishes. For all investigated cases, the amplitude of the transfer function of chemical potential is negligibly small. However, the amplitude of the transfer function for the mixture fraction is of considerable value, showing that mixture fraction is the only dominant contributor to the chemical mechanisms of entropy wave generation. Further, as predicted by Hield et al. [38], the peaks of heat release and pressure transfer functions occur at almost the same Strouhal number.

Expectedly, increasing the excess air results in higher amplitude of the mixture fraction fluctuations, while amplitudes of the other transfer functions remain almost unaffected. Increasing excess air in the lean combustion regime implies larger fuel mass fraction, which can introduce stronger variation in mass flow of the fuel. As the mixture fraction and fuel mass fraction are linearly related [68], the fluctuations in mixture fraction are quite pronounced. Pressure disturbances appear to be the most powerful mechanism of entropy wave generation at low frequencies ($St<1$), which can lead to the so-called Rumble instability [19,23,63], as also supported by Refs. [58,69]. However, at

higher frequencies ($St>10$) the generation of entropy wave becomes dominant by mixture fraction as the amplitude of transfer function of this quantity is up to three times larger than those of other sources. Further to $\phi h$, $\phi p$ and $\phi u$, having the characteristics of a low-pass filter, $\phi z$ represents similar response with a wider range of passing frequency. This is raised from the slow diffusion mechanism, which dominantly affects the mixture fraction variation and could be the reason for the domination of $\phi z$ at larger $St$. The cut-off frequency is slightly different amongst the various transfer functions (see Appendix C). The derived cut-off frequencies indicate that they are different from those presented by Karimi et al. [53] and Yoon [58], due to the involvement of chemical component of entropy wave. As also stated by Yoon [58], increasing the flame length increases the cut-off frequency regardless of the interactions amongst different sources of entropy generation.

Fig. 3 further presents the phases of transfer functions. The general trend of phase variations remains unchanged by increasing the excess air. The phase of the transfer function of mixture fraction is shifted towards lower values by approaching stoichiometric condition. However, the phase of transfer function for chemical potential shows an inverse trend in comparison with that of mixture fraction. Phase variation of the chemical transfer functions is strongly affected by the considerable changes in the chemical compositions of combustion products at different excess air values. Strong fluctuations of the phase at high frequencies is a result of significant dispersion of entropy wave [14,30]. In general, lower amplitudes of the transfer functions at high frequencies result in negligible contribution with the system behavior. An exception to this is the transfer function of mixture fraction that could be representative of the system response at high frequencies. The phase of velocity transfer function features a higher range of fluctuations than those of other transfer functions, showing the behavior of a non-minimum phase function [70]. It covers the entire range of phase variation and features a rapid response, which raises concerns for the control of combustion system [9]. Comparatively, the phase of chemical transfer functions, i.e. $\phi z$ and $\phi\Psi$, fluctuates considerably less. Slight phase variation can postpone the system response being on the opposite phase, which may completely change the dynamical behavior of the system.

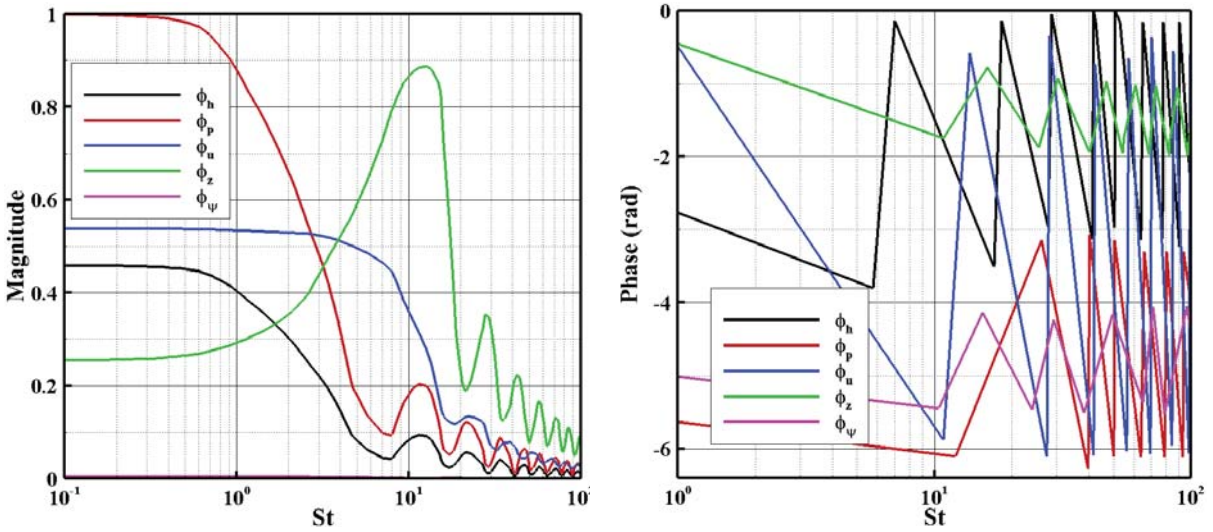


(a)

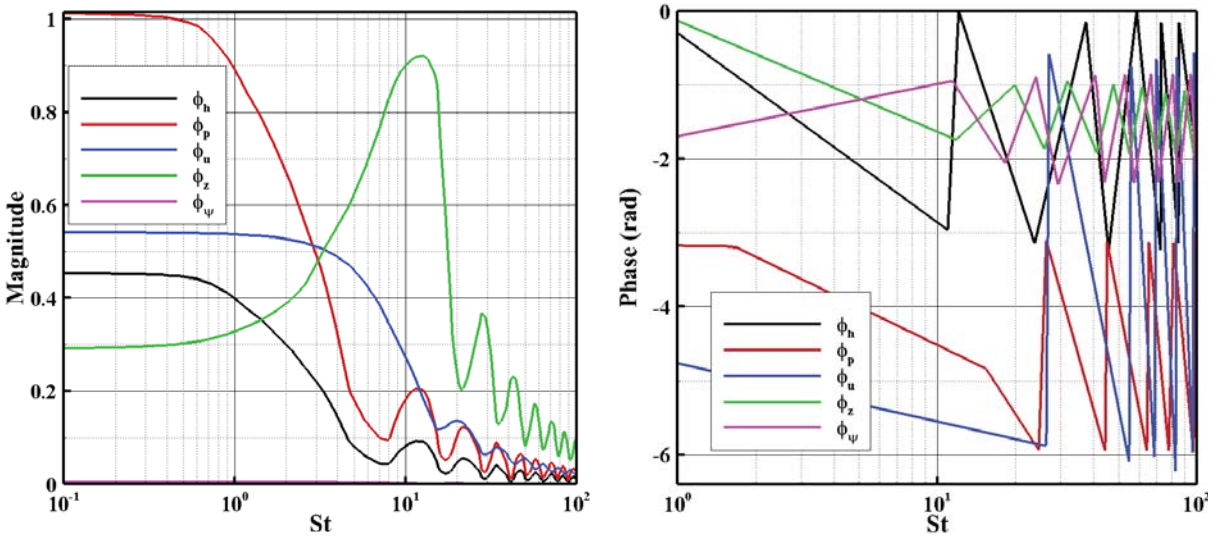


(b)

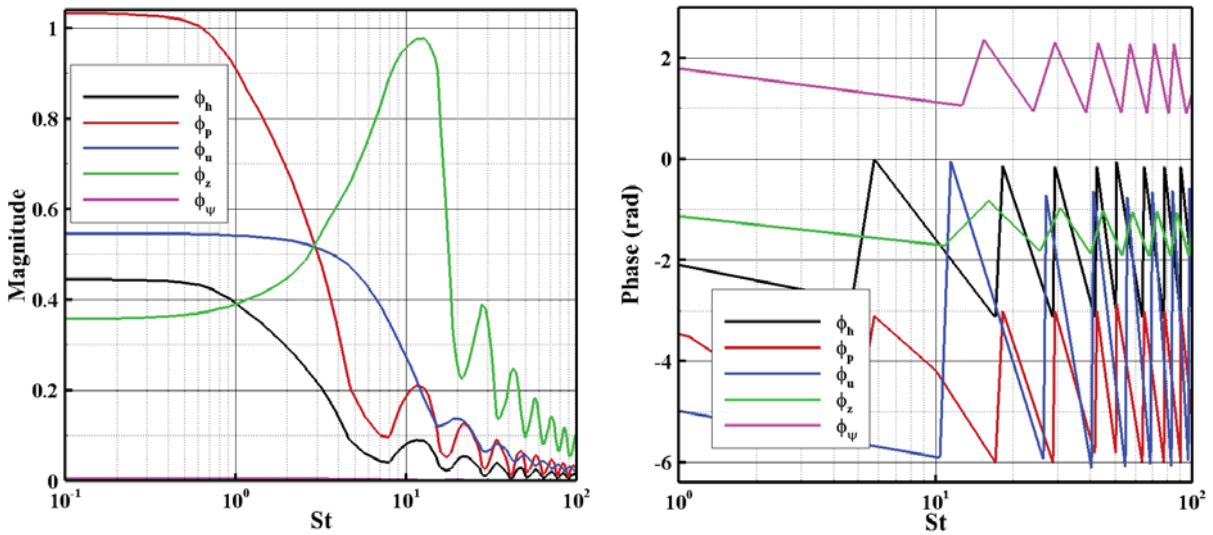


(c)

Fig. 3. Amplitude and phase of the transfer functions of entropy generation versus Strouhal number

for three values of excess air: (a) 25%, (b) 12% and (c) 0%.

Fig. 4 illustrates the amplitude of transfer functions, versus Strouhal number of resonance frequencies ($StR$), defined at the local maxima of the transfer function amplitude. Five different values of flame length between $\Delta=0.04$m and $\Delta=0.12$m have been investigated in this figure. To demonstrate the significance of variations, the flame lengths were chosen to be the same as those selected by Yoon [58]. Since $\phi\Psi$ has a negligibly small amplitude in the frequency domain (see Fig. 3), it has been excluded from Fig. 4. It is found that the resonance frequency is a complicated function of flame length and other chemical, thermal and hydrodynamic variables, as they can all potentially alter the system response. The low-pass filter characteristic of the transfer functions is, once again, apparent in this figure. Referring to Eq. (35), the same Strouhal number for cases with various flame length does not indicate the same frequency. Therefore, the amplitudes presented in Fig. 4 are not comparable at the same Strouhal numbers. Nonetheless, the decline of amplitude by increasing flame length is evident. Fig. 4 further confirms the major contribution of the mixture fraction fluctuations with the generation of entropy wave. Pressure, velocity and heat release fluctuations are respectively ranked as the next effective sources. Compared to those of other transfer functions, the mixture fraction and pressure show stronger dependency on the variations of flame length.

As already presented in Fig. 2, the energy of entropy wave has an inverse relation with the flame length. Making the flame length thinner from 0.12m down to 0.01m leads to the increment of the wave energy by a factor of 4.5. The thinner flame tends to resemble a theoretical impulse, exciting the responses at all frequencies [70]. This indicates that more energy, stored in a wide range of frequency spectrum, can be released by a thinner flame. The flame of higher excess air generates stronger entropy waves in the temporal domain. This is caused by intensifying the transfer function of mixture fraction, and confirms the substantial role of chemical transfer function in the wave response. It shows that the mixture fraction fluctuations can act as a dominant source of entropy waves, which then influence the process of conversion of entropic energy to acoustics. Thus, if neglected, it can render major errors in the low-order models and the subsequent stability analysis of the combustor.

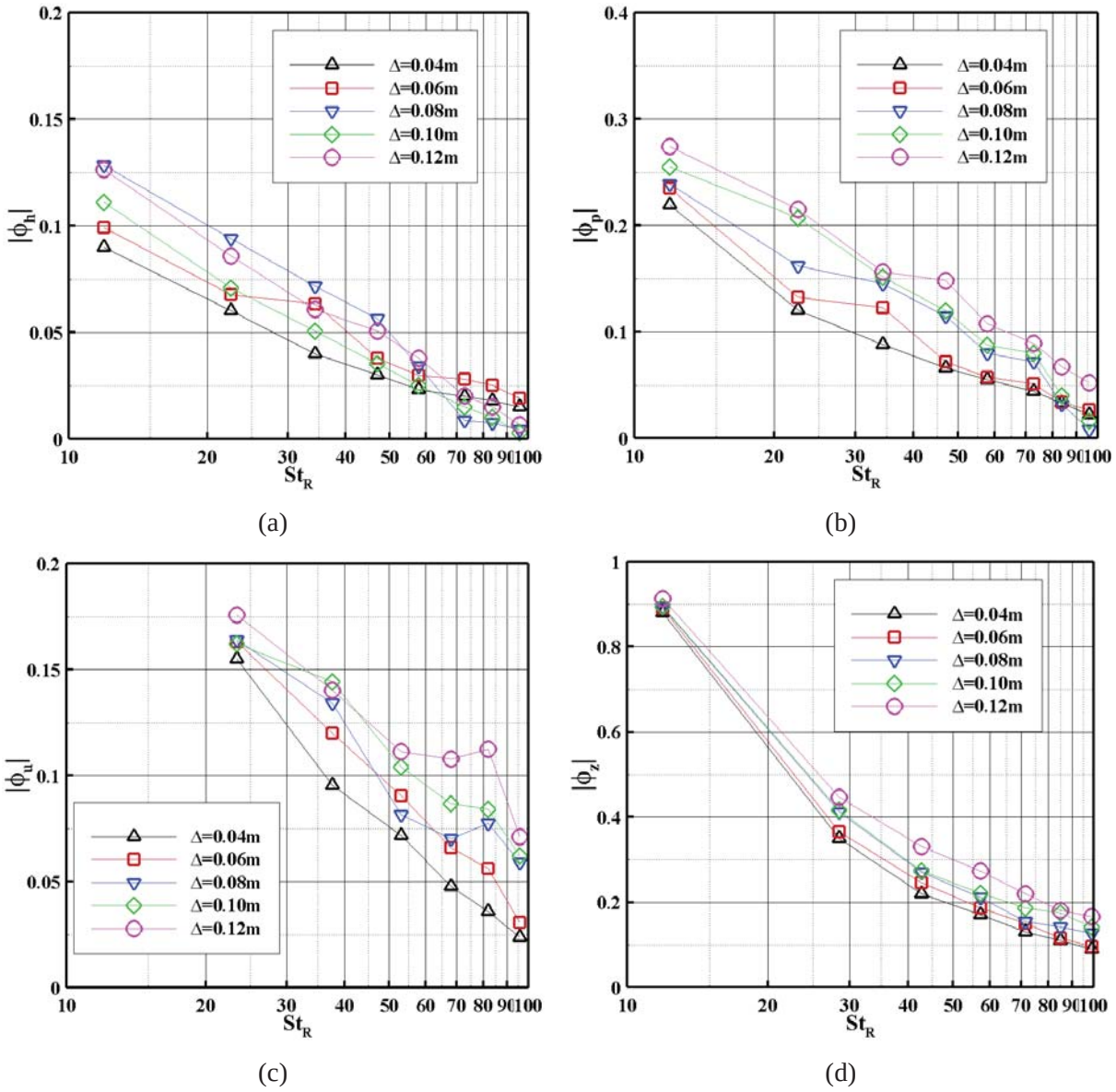


Fig. 4. Amplitude of entropy wave transfer functions at resonance Strouhal number at excess air of 25% for (a) heat release, (b) pressure, (c) velocity and (d) mixture fraction.

Assuming an infinitesimally thin flame leads to certain simplifications in solving the governing equations in the flame region. Most notably, it indicates that the flame length is much smaller compared to all other length scales in the reacting flow [71]. By approaching the limit of thin flame, the entropy wave becomes a time-invariant function. The flame thin limit is approached by $\Delta \rightarrow 0$ or $(m-1)u1\Delta \rightarrow \infty$, which means $St \rightarrow 0$, implying an acoustically compact region for the flame. Under the assumption of thin flame and employing Taylor series expansion, the transfer functions, presented in Eqs. (29) to (33), are reduced to the followings in which subscribe “TFL” denotes “thin flame limit”.

$$\phi h,TFL=\ln(m)m-1, \tag{36}$$

$$\phi p,TFL=(1\eta-1)\ln(m), \tag{37}$$

$$\phi u,TFL=(1m-1)(1\eta-1), \tag{38}$$

$$\phi \Psi,TFL=0, \tag{39}$$

$$\phi Z,TFL=0. \tag{40}$$

Fig. 5 shows that, for an infinitesimally thin flame and regardless of the temperature ratio, the magnitude of transfer function of heat release is by far larger than those of other two. Therefore, the major contribution of the transfer function of heat release with entropy generation of a thin flame is confirmed. The magnitude of all the transfer functions approach nearly the same value at higher values of temperature ratio. This is an indicator that a flame with high temperature ratio under the thin length assumption makes no relative extremum for any transfer function. The rate of magnitude change with temperature ratio is steeper for the pressure transfer function. This can be emanated from the direct effect of mean temperature variation on pressure fluctuations through the ideal gas law by considering constant value of mean pressure. Both pressure and velocity take the least values of magnitude. Further, the absence of chemical effects on the system response makes a thin flame different to a real flame. Comparing Figs. 3 and 5 illustrates higher amplitude of the transfer function of thin flame limit in comparison to those for flames with finite length. It follows that this assumption overestimates the energy contained in the flame, resulting in an unrealistic intensification of the transfer functions of entropy generation. Furthermore, although the absolute magnitudes are shown in Fig. 5, the values of pressure and velocity transfer function were found to be negative. This indicates that the pressure and velocity fluctuations unrealistically reduce the generation of unsteady entropy by the flame.

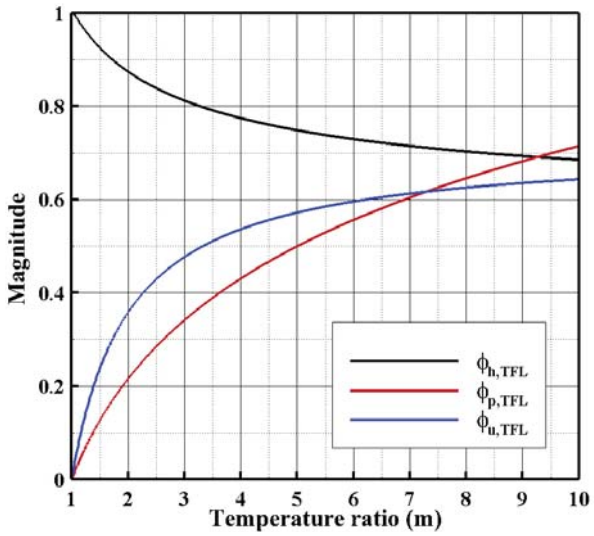


Fig. 5. Absolute values of the transfer function of entropy wave in the limit of thin flame.

## 6. Conclusions

A linear theory was developed to predict the dynamics of entropy wave generation. Transfer functions were derived analytically for the generation of entropy wave by chemical and non-chemical sources in a one-dimensional, laminar, ducted flow. The analysis assumed single-step and infinitely fast chemistry for a diffusion flame at Shvab-Zeldovich limit. The analytical results were validated against a computational model and it was shown that they could be reduced to the existing expressions for simpler configurations. This work extended a recent theoretical study on the generation of entropy waves [58] to include chemical sources and molecular diffusion. The key findings of the current study are summarized as follows.

- The analysis revealed that the fluctuations responsible for unsteady production of entropy are heat release, pressure, velocity, mixture fraction and chemical potential.
- All components of the transfer function of entropy wave generation appeared to have a low-pass filter character. Analysis of zeros of the transfer functions showed that the velocity-entropy decomposition could be important in the onset of combustion instability.
- Mixture fraction was found to be the most significant production source of entropy wave for $St>10$, while chemical potential had the least contribution over the entire frequency range. Ignoring mixture fraction as a source of entropy wave could result in the erroneous calculation of the unstable modes and incorrect prediction of entropy wave conversion.
- It was argued that thin flames produce unrealistically large entropy waves with the largest amplitude of transfer function of heat release.
- Consideration of the chemical sources of unsteady entropy generation led to variation of the entropic cut-off frequency. This reflects the importance of these sources in low-order modelling of indirect combustion noise and stability analysis of combustors.

- For $St<1$, the transfer functions of entropy waves downstream of the flame could be arranged from the highest to the lowest value by the inlet fluctuations in pressure, velocity, heat release and mixture fraction.

In future, the turbulent dissipation and shear dispersion of the entropy wave could be further added to the analysis.

## Data availability

The data that support the findings of this study are available from the corresponding author upon reasonable request.


### Acknowledgment

N. Karimi acknowledges the financial support of Engineering and Physical Science Research Council through grant EP/N020472/1.


## References


[1] Ihme, M., 2017. Combustion and engine-core noise. *Annual Review of Fluid Mechanics*, 49, pp.277-310. https://doi.org/10.1146/annurev-fluid-122414-034542.

[2] Muthukrishnan, M., Strahle, W.C. and Neale, D.H., 1978. Separation of hydrodynamic, entropy, and combustion noise in a gas turbine combustor. *AIAA Journal*, *16*(4), pp.320-327. https://doi.org/10.2514/3.60895.

[3] Marble, F.E. and Candel, S.M., 1977. Acoustic disturbance from gas non-uniformities convected through a nozzle. *Journal of Sound and Vibration*, *55*(2), pp.225-243. https://doi.org/10.1016/0022-460X(77)90596-X.

[4] Dowling, A.P. and Mahmoudi, Y., 2015. Combustion noise. *Proceedings of the Combustion Institute*, *35*(1), pp.65-100. https://doi.org/10.1016/j.proci.2014.08.016.

[5] Neise, W. and Enghardt, L., 2003. Technology approach to aero engine noise reduction. *Aerospace Science and Technology*, *7*(5), pp.352-363. https://doi.org/10.1016/S1270-9638(03)00027-0.

[6] Poinsot, T. and Veynante, D., 2005. *Theoretical and numerical combustion*. RT Edwards, Inc.

[7] Swaminathan, N. and Bray, K.N.C. eds., 2011. *Turbulent premixed flames*. Cambridge University Press. https://doi.org/10.1007/978-3-642-98027-5_14.

[8] Candel, S., 2002. Combustion dynamics and control: Progress and challenges. *Proceedings of the combustion institute*, *29*(1), pp.1-28. https://doi.org/10.1016/S1540-7489(02)80007-4.

[9] Lieuwen, T.C., 2012. *Unsteady combustor physics*. Cambridge University Press.

[10] Strahle, W.C., 1971. On combustion generated noise. *Journal of Fluid Mechanics*, *49*(2), pp.399-414.

[11] Cumpsty, N.A. and Marble, F.E., 1977. Core noise from gas turbine exhausts. *Journal of Sound and Vibration*, *54*(2), pp.297-309. https://doi.org/10.1016/0022-460X(77)90031-1.

[12] Karimi, N., Brear, M.J. and Moase, W.H., 2010. On the interaction of sound with steady heat communicating flows. *Journal of sound and vibration*, *329*(22), pp.4705-4718. https://doi.org/10.1016/j.jsv.2010.05.009.

[13] Morgans, A.S. and Duran, I., 2016. Entropy noise: A review of theory, progress and challenges. *International Journal of Spray and Combustion Dynamics*, *8*(4), pp.285-298. https://doi.org/10.1177/1756827716651791.

[14] Hosseinalipour, S.M., Fattahi, A. and Karimi, N., 2016. Investigation of the transmitted noise of a combustor exit nozzle caused by burned hydrogen-hydrocarbon gases. *International Journal of Hydrogen Energy*, *41*(3), pp.2075-2086. https://doi.org/10.1016/j.ijhydene.2015.10.119.

[15] Burnley, V.S. and C. Culick, F.E., 2000. Influence of random excitations on acoustic instabilities in combustion chambers. *AIAA journal*, *38*(8), pp.1403-1410. https://doi.org/10.2514/2.1116.

[16] Huang, Y. and Yang, V., 2009. Dynamics and stability of lean-premixed swirl-stabilized combustion. *Progress in energy and combustion science*, *35*(4), pp.293-364. https://doi.org/10.1016/j.pecs.2009.01.002.

[17] Keller, J.J., Egli, W. and Hellat, J., 1985. Thermally induced low-frequency oscillations. *Zeitschrift für angewandte Mathematik und Physik ZAMP*, *36*(2), pp.250-274.

[18] Dowling, A.P. and Stow, S.R., 2003. Acoustic analysis of gas turbine combustors. *Journal of propulsion and power*, *19*(5), pp.751-764. https://doi.org/10.1007/BF00945460.

[19] Polifke, W., Paschereit, C.O. and Döbbeling, K., 2001. Constructive and destructive interference of acoustic and entropy waves in a premixed combustor with a choked exit. *Int. J. Acoust. Vib*, *6*(3), pp.135-146. https://doi.org/10.20855/ijav.2001.6.382.

[20] Zhu, M., Dowling, A.P. and Bray, K.N.C., 2000. Self-excited oscillations in combustors with spray atomizers. *J. Eng. Gas Turbines Power*, *123*(4), pp.779-786. https://doi.org/10.1115/2000-GT-0108.

[21] Giuliani, F., Gajan, P., Diers, O. and Ledoux, M., 2002. Influence of pulsed entries on a spray generated by an air-blast injection device: An experimental analysis on combustion instability processes in aeroengines. *Proceedings of the combustion institute*, *29*(1), pp.91-98. https://doi.org/10.1016/S1540-7489(02)80016-5.

[22] Motheau, E., Nicoud, F. and Poinsot, T., 2014. Mixed acoustic–entropy combustion instabilities in gas turbines. *Journal of Fluid Mechanics*, *749*, pp.542-576. https://doi.org/10.1017/jfm.2014.245.

[23] Hochgreb, S., Dennis, D., Ayranci, I., Bainbridge, W. and Cant, S., 2013, June. Forced and self-excited instabilities from lean premixed, liquid-fuelled aeroengine injectors at high pressures and temperatures. In *ASME Turbo Expo 2013: Turbine Technical Conference and Exposition*. American Society of Mechanical Engineers Digital Collection. https://doi.org/10.1115/GT2013-95311.

[24] Stow, S.R., Dowling, A.P. and Hynes, T.P., 2002. Reflection of circumferential modes in a choked nozzle. *Journal of Fluid Mechanics*, *467*, pp.215-239. https://doi.org/10.1017/S0022112002001428.

[25] Goh, C.S. and Morgans, A.S., 2011. Phase prediction of the response of choked nozzles to entropy and acoustic disturbances. *Journal of Sound and Vibration*, *330*(21), pp.5184-5198. https://doi.org/10.1016/j.jsv.2011.05.016.

[26] Moase, W.H., Brear, M.J. and Manzie, C., 2007. The forced response of choked nozzles and supersonic diffusers. *Journal of Fluid Mechanics*, *585*, pp.281-304. https://doi.org/10.1017/S0022112007006647.

[27] Giauque, A., Huet, M. and Clero, F., 2012. Analytical analysis of indirect combustion noise in subcritical nozzles. *Journal of Engineering for Gas Turbines and Power*, *134*(11), p.111202. https://doi.org/10.1115/1.4007318.

[28] Duran, I. and Moreau, S., 2013. Solution of the quasi-one-dimensional linearized Euler equations using flow invariants and the Magnus expansion. *Journal of Fluid Mechanics*, *723*, pp.190-231. https://doi.org/10.1017/jfm.2013.118.

[29] De Domenico, F., Rolland, E.O. and Hochgreb, S., 2019. A generalised model for acoustic and entropic transfer function of nozzles with losses. *Journal of Sound and Vibration*, *440*, pp.212-230. https://doi.org/10.1016/j.jsv.2018.09.011.

[30] Fattahi, A., Hosseinalipour, S.M., Karimi, N., Saboohi, Z. and Ommi, F., 2019. On the response of a lean-premixed hydrogen combustor to acoustic and dissipative-dispersive entropy waves. *Energy*, *180*, pp.272-291. https://doi.org/10.1016/j.energy.2019.04.202.

[31] Leyko, M., Nicoud, F. and Poinsot, T., 2009. Comparison of direct and indirect combustion noise mechanisms in a model combustor. *AIAA journal*, *47*(11), pp.2709-2716. https://doi.org/10.2514/1.43729.

[32] Bake, F., Kings, N. and Roehle, I., 2008. Fundamental mechanism of entropy noise in aero-engines: Experimental investigation. *Journal of Engineering for Gas Turbines and Power*, *130*(1), p.011202. https://doi.org/10.1115/1.2749286.

[33] Bake, F., Richter, C., Mühlbauer, B., Kings, N., Röhle, I., Thiele, F. and Noll, B., 2009. The entropy wave generator (EWG): a reference case on entropy noise. *Journal of Sound and Vibration*, *326*(3-5), pp.574-598. https://doi.org/10.1016/j.jsv.2009.05.018.

[34] Fattahi, A., Hosseinalipour, S.M. and Karimi, N., 2017. On the dissipation and dispersion of entropy waves in heat transferring channel flows. *Physics of Fluids*, *29*(8), p.087104. https://doi.org/10.1063/1.4999046.

[35] Hosseinalipour, S.M., Fattahi, A., Afshari, H. and Karimi, N., 2017. On the effects of convecting entropy waves on the combustor hydrodynamics. *Applied Thermal Engineering*, *110*, pp.901-909. https://doi.org/10.1016/j.applthermaleng.2016.08.220.

[36] Moreau, S., Becerril, C. and Gicquel, L.Y.M., 2018. Large-Eddy-simulation prediction of indirect combustion noise in the entropy wave generator experiment. *International Journal of Spray and Combustion Dynamics*, *10*(2), pp.154-168. https://doi.org/10.1177/1756827717740775.

[37] Motheau, E., Nicoud, F. and Poinsot, T., 2014. Mixed acoustic–entropy combustion instabilities in gas turbines. *Journal of Fluid Mechanics*, *749*, pp.542-576. https://doi.org/10.1017/jfm.2014.245.

[38] Hield, P.A., Brear, M.J. and Jin, S.H., 2009. Thermoacoustic limit cycles in a premixed laboratory combustor with open and choked exits. *Combustion and Flame*, *156*(9), pp.1683-1697. https://doi.org/10.1016/j.combustflame.2009.05.011.

[39] Sattelmayer, T., 2002. Influence of the combustor aerodynamics on combustion instabilities from equivalence ratio fluctuations. *J. Eng. Gas Turbines Power*, *125*(1), pp.11-19. https://doi.org/10.1115/1.1365159.

[40] Morgans, A.S., Goh, C.S. and Dahan, J.A., 2013. The dissipation and shear dispersion of entropy waves in combustor thermoacoustics. *Journal of Fluid Mechanics*, *733*. https://doi.org/10.1017/jfm.2013.448.

[41] Eckstein, J., Freitag, E., Hirsch, C. and Sattelmayer, T., 2006. Experimental study on the role of entropy waves in low-frequency oscillations in a RQL combustor. *Journal of Engineering for Gas Turbines and Power*, *128*(2), pp.264-270. https://doi.org/10.1115/1.2132379.

[42] Eckstein, J. and Sattelmayer, T., 2006. Low-order modeling of low-frequency combustion instabilities in aeroengines. *Journal of propulsion and power*, *22*(2), pp.425-432. https://doi.org/10.2514/1.15757.

[43] Hosseinalipour, S.M., Fattahi, A., Khalili, H., Tootoonchian, F. and Karimi, N., 2020. Experimental investigation of entropy waves' evolution for understanding of indirect combustion noise in gas turbine combustors. *Energy*, *195*, p.116978. https://doi.org/10.1016/j.energy.2020.116978.

[44] Christodoulou, L., Karimi, N., Cammarano, A., Paul, M. and Navarro-Martinez, S., 2020. State prediction of an entropy wave advecting through a turbulent channel flow. *Journal of Fluid Mechanics*, *882*. https://doi.org/10.1017/jfm.2019.799.

[45] Sinai, Y.L., 1980. The generation of combustion noise by chemical inhomogeneities in steady, low-Mach-number duct flows. *Journal of Fluid Mechanics*, *99*(2), pp.383-397. https://doi.org/10.1017/S0022112080000663.

[46] Lighthill, M.J., 1952. On sound generated aerodynamically I. General theory. *Proceedings of the Royal Society of London. Series A. Mathematical and Physical Sciences*, *211*(1107), pp.564-587. https://doi.org/10.1098/rspa.1952.0060.

[47] Magri, L., O'Brien, J. and Ihme, M., 2016. Compositional inhomogeneities as a source of indirect combustion noise. *Journal of Fluid Mechanics*, *799*. https://doi.org/10.1017/jfm.2016.397.

[48] Magri, L., O'Brien, J. and Ihme, M., 2018. Effects of nozzle Helmholtz number on indirect combustion noise by compositional perturbations. *Journal of Engineering for Gas Turbines and Power*, *140*(3), p.031501. https://doi.org/10.1115/1.4037914.

[49] Rolland, E.O., De Domenico, F. and Hochgreb, S., 2018. Direct and indirect noise generated by entropic and compositional inhomogeneities. *Journal of Engineering for Gas Turbines and Power*, *140*(8), p.082604. https://doi.org/10.1115/1.4039050.

[50] Giusti, A., Magri, L. and Zedda, M., 2019. Flow Inhomogeneities in a Realistic Aeronautical Gas-Turbine Combustor: Formation, Evolution, and Indirect Noise. *Journal of Engineering for Gas Turbines and Power*, *141*(1), p.011502. https://doi.org/10.1115/1.4040810.

[51] Bloxsidge, G.J., Dowling, A.P., Hooper, N. and Langhorne, P.J., 1988. Active control of reheat buzz. *AIAA journal*, *26*(7), pp.783-790. https://doi.org/10.2514/3.9970.

[52] Dowling, A.P., 1995. The calculation of thermoacoustic oscillations. *Journal of sound and vibration*, *180*(4), pp.557-581. https://doi.org/10.1006/jsvi.1995.0100.

[53] Karimi, N., Brear, M.J. and Moase, W.H., 2008. Acoustic and disturbance energy analysis of a flow with heat communication. *Journal of Fluid Mechanics*, *597*, pp.67-89. https://doi.org/10.1017/S0022112007009573.

[54] Stow, S.R. and Dowling, A.P., 2009. A time-domain network model for nonlinear thermoacoustic oscillations. *Journal of engineering for gas turbines and power*, *131*(3), p.031502. https://doi.org/10.1115/GT2008-50770.

[55] Li, J. and Morgans, A.S., 2015. Time domain simulations of nonlinear thermoacoustic behaviour in a simple combustor using a wave-based approach. *Journal of Sound and Vibration*, *346*, pp.345-360. https://doi.org/10.1016/j.jsv.2015.01.032.

[56] Chen, L.S., Bomberg, S. and Polifke, W., 2016. Propagation and generation of acoustic and entropy waves across a moving flame front. *Combustion and Flame*, *166*, pp.170-180. https://doi.org/10.1016/j.combustflame.2016.01.015.

[57] Strobio Chen, L., Steinbacher, T., Silva, C. and Polifke, W., 2016. On generation of entropy waves by a premixed flame. In *ASME Turbo Expo 2016: Turbomachinery Technical*

*Conference and Exposition*. American Society of Mechanical Engineers Digital Collection. https://doi.org/10.1115/GT2016-57026.

[58] Yoon, M., 2020. The entropy wave generation in a heated one-dimensional duct. *Journal of Fluid Mechanics*, *883*. https://doi.org/10.1017/jfm.2019.901.

[59] Law, C.K., 2010. Combustion physics. Cambridge university press.

[60] Smolke, J., Carbone, F., Egolfopoulos, F.N. and Wang, H., 2018. Effect of n-dodecane decomposition on its fundamental flame properties. *Combustion and Flame*, *190*, pp.65-73.

[61] Noury, K. and Yang, B., 2019, November. Analytical statistical study of linear parallel feedforward compensators for non minimum-phase systems. In *ASME 2019 Dynamic Systems and Control Conference*. American Society of Mechanical Engineers Digital Collection. https://doi.org/10.1115/DSCC2019-9126.

[62] Sarkar, B.N., 2013. *Advanced Control Systems*. PHI Learning Pvt. Ltd..

[63] Goh, C.S. and Morgans, A.S., 2013. The influence of entropy waves on the thermoacoustic stability of a model combustor. *Combustion Science and Technology*, *185*(2), pp.249-268. https://doi.org/10.1080/00102202.2012.715828.

[64] Boashash, B., Touati, S., Flandrin, P., Hlawatsch, F., Taubock, G., Oliveira, P.M., Barroso, V., Baraniuk, R., Jones, G., Matz, G. and Alieva, T., 2015. Advanced time-frequency signal and system analysis. https://doi.org/10.1016/B978-0-12-398499-9.00004-2.

[65] Dowling, A.P., 1997. Nonlinear self-excited oscillations of a ducted flame. *Journal of fluid mechanics*, *346*, pp.271-290. https://doi.org/10.1017/S0022112097006484.

[66] Fleifil, M., Annaswamy, A.M., Ghoneim, Z.A. and Ghoniem, A.F., 1996. Response of a laminar premixed flame to flow oscillations: A kinematic model and thermoacoustic instability results. *Combustion and flame*, *106*(4), pp.487-510. https://doi.org/10.1016/0010-2180(96)00049-1.

[67] Chaparro, A., Landry, E. and Cetegen, B.M., 2006. Transfer function characteristics of bluff-body stabilized, conical V-shaped premixed turbulent propane–air flames. *Combustion and flame*, *145*(1-2), pp.290-299. https://doi.org/10.1016/j.combustflame.2005.10.013.

[68] Poinsot, T.J. and Veynante, D.P., 2018. Combustion. Encyclopedia of Computational Mechanics Second Edition, pp.1-30. https://doi.org/10.1002/9781119176817.ecm2067.

[69] Wassmer, D., Schuermans, B., Paschereit, C.O. and Moeck, J.P., 2017. Measurement and modeling of the generation and the transport of entropy waves in a model gas turbine combustor. International Journal of Spray and Combustion Dynamics, 9(4), pp.299-309. https://doi.org/10.1177/1756827717696326.

[70] Newland, D.E., 2012. *An introduction to random vibrations, spectral & wavelet analysis*. Courier Corporation. https://doi.org/10.3233/SAV-1994-1608.

[71] Kuo, K.K.Y. and Acharya, R., 2012. *Fundamentals of turbulent and multiphase combustion*. John Wiley & Sons. https://doi.org/10.1002/9781118107683.

**Appendix A: Numerical procedure**

The governing unsteady equations of continuity of mass, momentum and energy as well as conservation of species were discretized using a second order scheme for spatial and temporal terms. The two-dimensional computational domain was depicted in Fig. 1, bounded with two parallel adiabatic and solid walls with no-slip velocity boundary conditions. In this configuration, air continuously enters the channel under laminar flow regime with Reynolds number of 1000 and it is assumed that the flow is discharged to the ambient environment. A hot pocket of the combustion products of n-dodecane is injected into the channel at the moment that the air flow is completely zero, with a temporal width that makes the spatial value of $\Delta$, shown in Fig. 1. The products correspond to lean combustion of the fuel, with excess air values of 25%, 12% and 0. The computational grid consisted of 88000 cells, determined through grid independency tests. PISO algorithm was adopted to couple the velocity and pressure fields through using a finite volume method. The simulation was ran for five times of the flow residence time to ensure the washout of any transience before introducing the hot and compressed pocket of combustion products.

**Appendix B: Reducing the transfer functions for a single component fluid flow**

In this appendix, it is shown that the derived equations in Sections 2 and 3 can be reduced to those presented by Yoon [58] for single species fluid flow. As Yoon [58] did not consider combustion product for the flame region, gas constant is completely fixed in the flame region. That is $R1=R2$ and therefore, $\rho 2\rho 1=T1T2$. According to Eq. (7), $\kappa=-1\Delta ln\rho 2\rho 1$, and by incorporation of Taylor series, it turns into $\kappa=1\Delta\rho 1\rho 2-1=1\Delta T2T1-1$. Further, Eq. (21) yields $fT1=1\Delta T2T1-1$. This concludes that $\kappa=fT1$ and subsequently the non-chemical transfer functions, $\phi h$, $\phi p$ and $\phi u$, presented in Eqs. (29) to (31) reduce to those presented in the work of Yoon [58].

**Appendix C: Cut-off frequencies**

Conventionally, the cut-off frequency is found if the transfer function magnitude meets the value of 0.707 or -3db [62]. However, in the current work, the entropic cut-off frequency is simply obtained using the zeros, due to the monotonic decrease in the transfer function approaching $\omega c$, similar to Ref. [58]. Therefore, they give

$$\omega c,h=\omega c,p=T1[ku1\ln m-mku1-r\ln m+ku1]-fu1\ln mu1+fmu1-fu1T1\ln m,$$

$$\omega c,Z=-T1r\ln m+u1f\ln m-u1fm+u1fT1\ln m,$$

$\omega c, Z = 12mT1\ln mku1mT1\ln m - fu1ml nm - mrT1 + \ln m2T12k2m2u12 - 2\ln m2m2u12fkT1 + \ln m2T12f2m2u12 + 2\ln mT12m2rku1 - 2\ln mm2T1fru1 - 4T12m2kru1 + 4T12mkru1 + 5T12m2r2 + 4T1fru1m2 - 4T12r2m - 4T1fru1m12.$

To find these frequencies, Taylor series expansion is applied. The cut-off frequency for the chemical potential is not presented here, as its amplitude takes the lowest values that are near zero (see Fig. 3).